Int J Ind Chem (2016) 7:231–240
DOI 10.1007/s40090-016-0080-1

RESEARCH

Sorption behavior of some lanthanides on polyacrylamide stannic molybdophosphate as organic–inorganic composite

E. A. Abdel-Galil[1] · A. B. Ibrahim[1] · M. M. Abou-Mesalam[1]

Received: 9 March 2015 / Accepted: 15 April 2016 / Published online: 7 June 2016

Abstract Sorption behavior of some lanthanide ions such as lanthanum and samarium ions on polyacrylamide stannic molybdophosphate {PASnMoP} as organic–inorganic composite has been investigated. The distribution coefficients of La^{3+} and Sm^{3+} ions in different pH media on PASnMoP were determined with the selectivity order $La^{3+} > Sm^{3+}$. Capacity of PASnMoP for La^{3+} and Sm^{3+} ions was determined and found 24.66 and 15.38 mg g^{-1} for La^{3+} and Sm^{3+} ions, respectively. The resin dosage dependence for the sorption behavior for La^{3+} and Sm^{3+} ions on polyacrylamide stannic molybdophosphate was conducted. The adsorption isotherms were described by means of Langmuir and Freundlich isotherms for La^{3+} and Sm^{3+} ions. The Langmuir model represented the adsorption process better than the Freundlich model. The kinetic data were tested using Logergren-first-order and Pseudo-second-order kinetic models. The data correlated well with the Pseudo-second-order kinetic model, indicating that the chemical adsorption was the rate limiting step. Thermodynamic parameters $\Delta G°$, $\Delta H°$ and $\Delta S°$ were also calculated and the data showed that the ion exchange of La^{3+} and Sm^{3+} ions on PASnMoP was spontaneous and endothermic in nature.

Keywords Distribution coefficient · Lanthanides · Sorption isotherm · Polyacrylamide stannic molybdophosphate · Composite · Thermodynamic

✉ E. A. Abdel-Galil
ezzat_20010@yahoo.com

[1] Atomic Energy Authority, Hot Labs. Center, P.O. 13759, Cairo, Egypt

Introduction

Rare earth elements (REE) have been increasingly used in the field of chemical engineering, nuclear energy, optical, magnetic, luminescence and laser materials, high-temperature superconductors, secondary batteries and catalysis [1–6]. Lanthanum, one of the most abundant of the lanthanides, is an important element of mischmetal and hydrogen-absorbing alloy [3], Neodymium is the raw material used in high-strength permanent magnets (Nd-B-Fe), making it less expensive than samarium-cobalt permanent magnets [7]. Yttrium is an important element and in great demand in astronavigation, luminescence, nuclear energy and metallurgical industries [8]. Organic polymers as ion exchangers are well known for their uniformity, chemical stability and control of their ion-exchange properties through synthetic methods. The inorganic ion-exchange materials besides other advantages are important in being more stable to high temperature and radiation field than the organic ones [9]. To obtain a combination of these advantages associated with polymeric and inorganic materials as ion exchangers, attempts have been made to develop polymeric–inorganic composite ion exchangers by incorporation of organic monomers in the inorganic matrix [10]; few such excellent ion-exchange materials have been developed and are successfully being used in chromatographic techniques [11–13].

In the present work, polyacrylamide stannic molybdophosphate was synthesized as reported earlier [14]. Distribution coefficient and separation factors (∝) of La^{3+} and Sm^{3+} on polyacrylamide stannic molybdophosphate were determined. Capacity, sorption isotherms and thermodynamic parameters have been calculated for the sorption of La^{3+} and Sm^{3+} ions on polyacrylamide stannic molybdophosphate.

Materials and methods

All reagents and chemicals were of analytical grade purity and used without further purification. pH measurements were performed using pH meter of the bench, model 601A, USA. The concentration of La^{3+} and Sm^{3+} ions in solutions was measured by UV spectrophotometer UV-1700.

Polyacrylamide stannic molybdophosphate {PASnMoP} as organic–inorganic composite was prepared as described earlier by Abdel-Galil [14]. Polyacrylamide was prepared by mixing equal volume of acrylamide and potassium persulfate. A viscous solution was obtained by heating the mixture gently at 70 °C with continuous stirring. Inorganic precipitate of Sn(IV) molybdophosphate was prepared at 25 °C by mixing equal volumes of the solutions of stannic chloride (0.1 M), ammonium molybdate (0.1 M) and orthophosphoric acid (1 M). The yellow precipitate was obtained when the pH of the mixture was adjusted to 1.05 by adding aqueous ammonia (NH_4OH). The viscous solution of polyacrylamide was added to the yellow inorganic precipitate of Sn(IV) molybdophosphate and mixed thoroughly with continuous stirring. The resultant yellow colored slurry was refluxed for 3 h at a temperature of 70 ± 5 °C and the color of the slurry changed from yellow to greenish color. The resultant greenish colored slurry was kept for 24 h at room temperature for digestion. The supernatant liquid was decanted and gel was filtered using a centrifuge (about 10^4 rpm) and dried at 50 ± 1 °C. The product was crashed to obtain small granules and converted to H^+-form by treating with 1 M HNO_3 for 24 h with occasional shaking intermittently replacing the supernatant liquid with fresh acid and the color of the product became yellow. The excess acid was removed after several washing with DMW, dried at 50 °C and sieved to obtain particles of particular size range (0.115–0.375 mm). The percentage of yield and physical appearance of beads were selected for further studies.

Sorption studies

The distribution coefficients (k_d) of La^{3+} and Sm^{3+} ions on polyacrylamide Sn(IV) molybdophosphate were determined by batch equilibration technique, as a function of different pH values. 0.1 g of {PASnMoP} was shaken with 10 ml of 50 ppm of La^{3+} and Sm^{3+} ions solution at V/m ratio of 100 ml/g. The mixture was placed overnight (sufficient to attain the equilibrium) in a shaker thermostat adjusted at 25, 45 or 65 ± 1 °C. After equilibrium, the solutions were separated by centrifugation and the concentration of La^{3+} and Sm^{3+} ions in the solution was determined using UV spectrophotometer. The pH values of the solutions were measured before and after equilibrium using pH meter. The distribution coefficient (k_d) and separation factor (∝) were evaluated by;

$$k_d = \frac{A_o - A_f}{A_f} \times \frac{V}{m} (\text{ml/g}) \quad (1)$$

$$\propto = \frac{(k_d)A}{(k_d)B} \quad (2)$$

where A_o is the concentration of the ions in solution before equilibrium, A_f is the concentration of the ions in solution after equilibrium, V is the volume of the solution (ml), m is the weight of the exchanger (g), and ∝ is the separation factor between two neighboring ions A and B.

Capacity measurements

The capacity of polyacrylamide stannic(IV) molybdophosphate for La^{3+} and Sm^{3+} ions was determined by the repeated batch technique, by equilibrating 0.05 g of PASnMoP ion exchanger with 5 ml of 100, 200, 400, 600, 800 and/or 1000 ppm of La^{3+} and/or Sm^{3+} ion solutions on a shaker thermostat adjusted at 25 ± 1 °C. After equilibrium, the solution was separated and repeated until no further sorption occurs. The capacity was calculated using the following equation:

$$\text{Capacity} = \text{Uptake} \times \frac{V}{m} \times C_o \text{ mg/g} \quad (3)$$

where C_o is the initial ion concentration in solution, V is the solution volume (ml) and m is the weight of the exchanger (g).

Adsorption isotherm

The adsorption isotherms were done, as it is well known, by a gradual increase in the concentration of sorbate ion in solution and measuring the amount sorbed at each equilibrium concentration. The degree of sorption showed therefore is a function of the concentration of sorbate ions only. The adsorption isotherms were carried out with different initial concentrations varying from 100 to 1000 ppm at different reaction temperatures 25, 45 and/or 65 ± 1 °C and at constant V/m value of 100 ml/g and pH 3. After equilibrium, the respective mixture was filtered and then the concentration of La^{3+} and Sm^{3+} was measured.

Kinetic measurements

The kinetic analysis of the adsorption process for La^{3+} and Sm^{3+} ions on polyacrylamide stannic(IV) molybdophosphate was carried out by mixing the exchanger with metal ions solution at 50 ppm with a V/m ratio of 100 ml/g in a shaker thermostat at 25 ± 1 °C. The solution was separated at different time intervals and analyzed to determine

the metal ion concentration in solution using UV spectrophotometer for La^{3+} and Sm^{3+}. The extent of sorption was determined from the equation.

$$\text{Sorption } \% = \{(A_i - A_f)/A_i\} \times 100 \quad (4)$$

where A_i and A_f are the initial and final concentrations of metal ions in solution.

Results and discussion

Polyacrylamide stannic molybdophosphate as organic–inorganic cation exchange material was prepared as described earlier by Abdel-Gelil [14].

The influence of adsorbent dosage on the adsorption of La^{3+} and Sm^{3+} was studied and the data are shown in Fig. 1. The adsorption of the metals increased with increasing the dosage of the exchanger. This increasing may be related to the increase in the surface area of the exchanger by increasing the adsorbent dosage, so more available active sides on the adsorbent and thus making easier penetration of metal ions to the sorption sides [15]. The data also indicate that the adsorption was almost constant at higher dosage than 0.1 g and the optimum dosage used in all investigation was 0.1 g with batch factor 100 ml/g.

The cation exchange process between H^+ (solid phase) and H^+ in solution can be represented by the following reaction:

$$nH^+ + M^{n+} ==== \overline{M^{n+}} + nH^+ \quad (5)$$

where a bar over a character denotes the concentration of M^{n+} on the solid and unbar denotes the concentration of M^{n+} in the solution phase.

The distribution coefficient (k_d) values are defined by the following relation:

$$k_d = \frac{[\overline{M^{n+}}]}{[M^{n+}]} \quad (6)$$

The selectivity K_H^M can be defined by the following equation:

$$K_H^M = \frac{[M^{n+}][H^+]^n}{[H^+][M^{n+}]} \quad (7)$$

From Eqs. (6 and 7), the distribution coefficient (k_d) can be written in the simple form as follows:

$$k_d = K_H^M \times \frac{[\overline{H^+}]^n}{[H^+]^n} \quad (8)$$

(or)

$$\log k_d = \log K_H^M \times [\overline{H^+}]^n - n \log[H^+] \quad (9)$$

From very dilute solutions, the activity coefficient in solution is very small and can be neglected, then

$$[\overline{M^{n+}}] << [\overline{H^+}] \quad \text{and} \quad [M^{n+}] << [H^+]$$

Then, the term $\log K_H^M \times [\overline{H^+}]$ is considered as constant and, thus, Eq. (9) can be reduced in the following form:

$$\text{Log } k_d = -n\log[H^+] = n \text{ pH} \quad (10)$$

When log k_d values are plotted against log pH, a straight line with slope n obtained, where n is refer to the valance of the sorbed ions. Figure 2 and Table 1 show the dependency of k_d values of La^{3+} and Sm^{3+} ions onto PASnMoP on the pH of the ion medium. The linear relationships between log k_d and pH values were observed for La^{3+} and Sm^{3+} ions with slopes 0.246 and 0.182, respectively. These slopes did not equal to the valence of the metal ions sorbed which

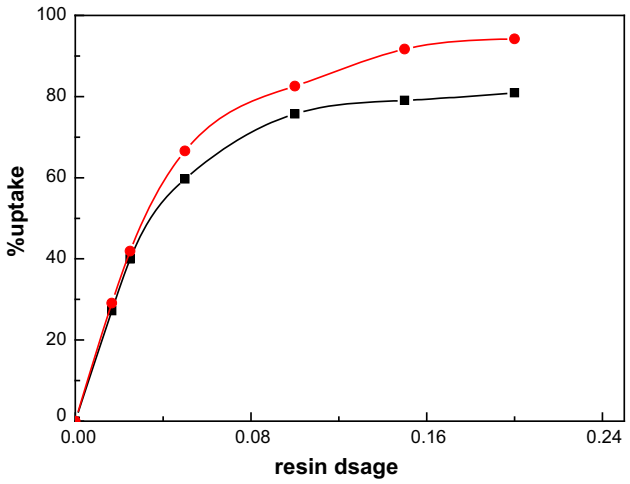

Fig. 1 Effect of ion exchanger dosage on sorption of Sm^{3+} and La^{3+} on {PASnMoP}

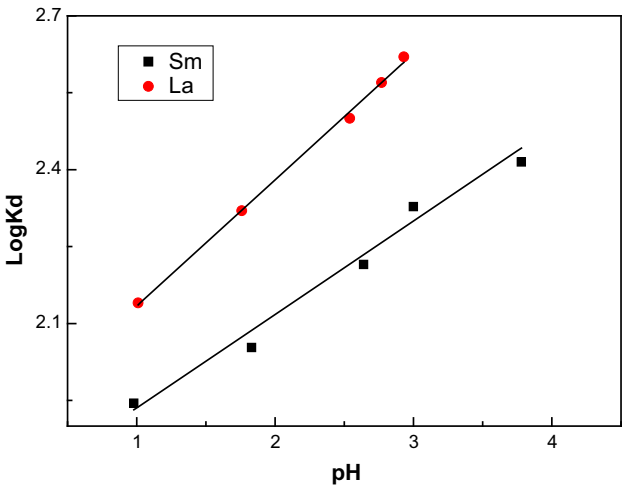

Fig. 2 Log k_d of La^{3+} and Sm^{3+} ions versus pH on {PASnMoP}

Table 1 K_d and separation factor values for La^{3+} and Sm^{3+} ions on PASnMoP

pH	k_d, ml/g (separation factor, ∝)	
	La^{3+}	Sm^{3+}
0.98	134.89	87.096
		(1.548)
1.69	199.53	114.82
		(1.737)
2.49	316.23	158349
		(1.995)
2.72	363.08	177.83
		(2.042)
2.90	398.11	190.55
		(2.089)

prove the non-ideality of the exchange reaction between La^{3+} and Sm^{3+} ions and PASnMoP. These findings cannot be explained only in terms of electrostatic interaction between the hydrated cations and the anionic sites in the exchanger. It may, therefore, be considered that the dependence of k_d for cations cannot be understood by a purely columbic interaction with the anionic sites, but also may be due to the formation of a covalent bond similar to a weakly acidic resin; such interaction would be closely related to the ionic potential of the cations [14].

The k_d values and separation factors of La^{3+} and Sm^{3+} ions in different pH on PASnMoP are summarized in Table 1. From the data in Table 1, we found that the selectivity order of the investigated cations on PASnMoP in the same conditions has the following sequence; $La^{3+} > Sm^{3+}$. This selectivity sequence is in accordance with the ionic radii; the ions with smaller ionic radii easily exchanged and move faster than the ions with greater ionic radii [14]. Also from Table 1, the separation factors between La^{3+} and Sm^{3+} metal ions on PASnMoP are relatively high and predict some selective separation of these ions which were available on PASnMoP.

Figures 3 and 4 show the k_d values for La^{3+} and Sm^{3+} ions, respectively, in different media at different reaction temperatures. The effect of reaction temperature on the adsorption was carried out in the temperature range 25–65 ± 1 °C. From these figures, we found that the K_d values are increased for La^{3+} and Sm^{3+} ions on PASnMoP with increasing the reaction temperature from 25 to 65 ± 1 °C. This behavior may be due to the endothermic nature of the system for the reaction of La^{3+} and Sm^{3+} ions on PASnMoP. Also, the increasing k_d with increasing the reaction temperatures may be attributed to the increasing mobility of La^{3+} and Sm^{3+} ions with increasing the reaction temperature [16]. Similar results were obtained by Abou-Mesalam et al. for the distribution coefficients of

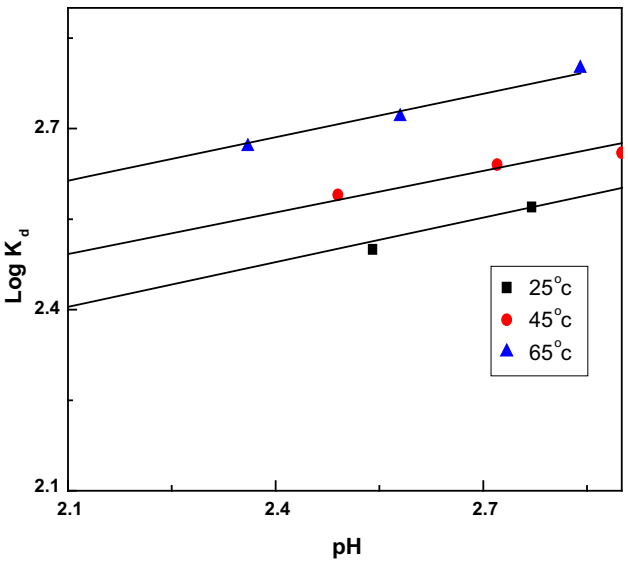

Fig. 3 Log k_d of La^{3+} ion as a function of pH on PASnMoP at different reaction temperatures

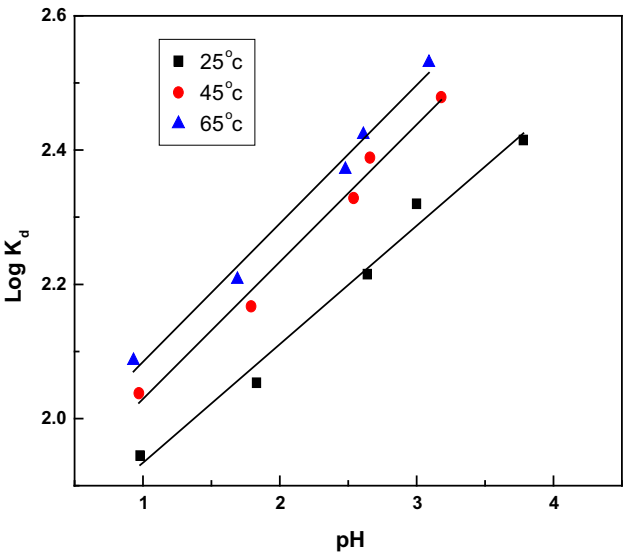

Fig. 4 Log k_d of Sm^{3+} ion as a function of pH on PASnMoP at different

^{22}Na, ^{60}Co and $^{152,154}Eu$ ions on titanium antimonate [17–19].

Figure 5 shows the linear relation between in k_d of La^{3+} and Sm^{3+} ions on PASnMoP and 1/T according to the Van't Hoff relation [17];

$$\ln k_d = \frac{\Delta S^o}{T} - \frac{\Delta H^o}{RT} \quad (11)$$

where $\Delta S°$ is the entropy change of adsorption, $\Delta H°$ is the enthalpy change of adsorption, R is the gas constant, and T is the absolute temperature.

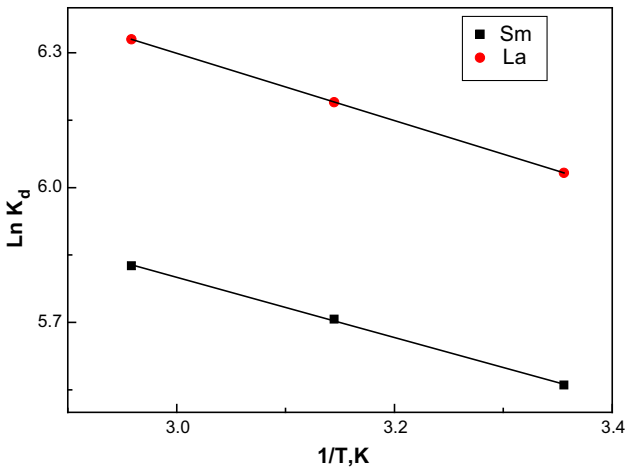

Fig. 5 Van't Hoff plot of the adsorption of La^{3+} and Sm^{3+} ions on PASnMoP

Table 2 Thermodynamic parameters for adsorption of La^{3+} and Sm^{3+} ions on PASnMoP

Metal	Temp.	ΔG^{o}	ΔH^{o}	ΔS^{o}
La^{3+}	298	−14.93	14.32	98
	318	−16.36		96
	338	−17.78		94.9
Sm^{3+}	298	−13.77	12.79	89
	318	−15.08		87
	338	−16.37		86

It was found that the distribution coefficient of La^{3+} and Sm^{3+} ions increased with increasing temperature from 298 to 338°K (i.e., the distribution coefficient decreased with increasing $1/T$) as shown in Fig. 5. This increase in the extent of adsorption with the increase in temperature was attributed to acceleration of some originally slow adsorption steps and creation of some new active sites on the adsorbent surfaces [20, 21]. From the slopes and intercepts of these straight lines represented in Fig. 5, the enthalpy change of adsorption ($\Delta H°$) and entropy change of adsorption ($\Delta S°$) were evaluated and represented in Table 2.

As shown in Table 2, the positive values of ($\Delta H°$) indicate the endothermic nature of the adsorption process [14]. The positive values of $\Delta S°$ indicate that the increased randomness of solid solution interface during the adsorption of these cations on PASnMoP [16]. The data in Table 2 indicate that the values of $\Delta H°$ for La^{3+} and Sm^{3+} ions on PASnMoP are greater than 12.6 KJmol^{-1} which indicated the presence of other mechanism for the adsorption of La^{3+} and Sm^{3+} ions on PASnMoP beside ion-exchange mechanism [22, 23]. These results are supported also from the data of K_d where the slope of the linear relationship between K_d and pH is not equal to the valence of La^{3+} and Sm^{3+} ions.

Table 3 Capacity of PASnMoP for La^{3+} and Sm^{3+} ions at 25 ± 1 °C

Concentration, mg/L	Capacity, mg/g	
	La^{3+}	Sm^{3+}
100	19.49	17.34
200	37.88	31.29
400	63.48	54.98
600	82.74	69.86
800	97.07	77.85
1000	98.85	77.69

The free energy change of specific adsorption $\Delta G°$ was calculated using the relation:

$$\Delta G^{o} = \Delta H^{o} - T\Delta S^{o} \quad (12)$$

and

$$\Delta G^{o} = RT \ln k_d \quad (13)$$

The negative values of free energy change $\Delta G°$ represented in Table 2 indicate that the adsorption process is spontaneous and indicates the preferable adsorption of these cations on PASnMoP compared with H^{+} ion [14, 16].

The capacity of PASnMoP for La^{3+} and Sm^{3+} ions was studied and the data are tabulated in Table 3. From Table 3, it is clear that the capacity of polyacrylamide Sn(IV) molybdophosphate samples for La^{3+} and Sm^{3+} has the following order: $La^{3+} > Sm^{3+}$. This sequence is in accordance with the hydrated radii of the exchanged ions. The ions with smaller hydrated radii enter the pores of the exchanger, resulting in higher adsorption [24, 25].

Sorption isotherm

Sorption equilibrium is usually described by an isotherm equation whose parameters express the surface properties and affinity of the sorbent, at a fixed temperature and pH. An adsorption isotherm describes the relationship between the amount of adsorbate on the adsorbent and the concentration of dissolved adsorbate in the liquid at equilibrium [26]. Langmuir and Freundlich isotherms are Komman kinds of several isotherm equations that were tested to fit the obtained sorption data.

The Langmuir adsorption model assumes that molecules are adsorbed at fixed number of well-defined sites, each of which can only hold one molecule and no trans-migration of adsorbate in the plane of the surface. These sites are also assured to be energetically equivalent and distant to each other, so there are no interactions between the molecules

adsorbed to adjacent sites. The linear form of the Langmuir isotherms is represented by the following equation [27]:

$$\frac{C_e}{q_e} = \frac{C_e}{q_m} + \frac{1}{K_L q_m} \quad (14)$$

where C_e is the equilibrium concentration of the metal (mg/L) and q_e is the amount of the metal adsorbed (mg) by per unit of the adsorbent (g). q_m and K_L are Langmuir constants relating adsorption capacity (mg/g) and the energy of adsorption (L/g), respectively, and evaluated from slope and intercept of the linear plots of C_e/q_e versus C_e, respectively.

The linearized Langmuir adsorption of La^{3+} and Sm^{3+} is given in Figs. 6 and 7. The Langmuir adsorption constants evaluated from isotherms and their correlation coefficient are presented in Table 4; it is clear that the Langmuir isotherm model provides an excellent fit to the equilibrium adsorption data, giving correlation coefficient of 0.994 for La^{3+} and 0.980 for Sm^{3+}, respectively.

Based on the further analysis of Langmuir equation, the dimensionless parameter of the equilibrium or adsorption intensity (R_L) can be expressed by

$$R_L = \frac{1}{1 + K_L C_o} \quad (15)$$

where C_o (mg L^{-1}) is the initial amount of adsorbate.

The R_L parameter is considered as more reliable indicator of the adsorption. There are four probabilities for the R_L value: (1) for favorable adsorption, $0 < R_L < 1$, (2) for unfavorable adsorption, $R_L > 1$, (3) for linear adsorption, $R_L = 1$, and (4) for irreversible adsorption, $R_L = 0$.

The variation of R_L with the initial metal concentration of solution is shown in Fig. 8. R_L values were found to be between 0 and 1 for all concentrations of La^{3+} and Sm^{3+}

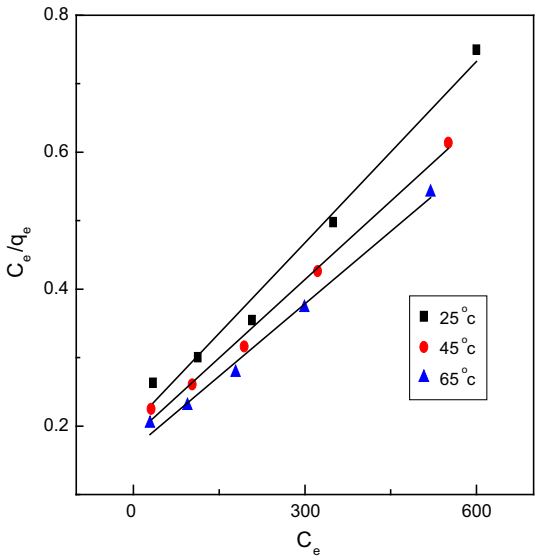

Fig. 7 Langmuir isotherm plot for the adsorption of Sm^{3+} onto {PASnMoP}

Table 4 Parameters of Langmuir isotherm for ion exchange of La^{3+} and Sm^{3+} on PASnMoP

Metal	T °K	q_m	R_L	K_L	Ln b	R^2
La^{3+}	298	14.43	0.147	0.0057	−5.15	0.9946
	318	15.1	0.131	0.0066	−5.01	0.9977
	338	15.4	0.114	0.0077	−4.85	0.9984
Sm^{3+}	298	4.922	4.34×10^{-6}	230.34	5.43	0.9800
	318	5.40	4.11×10^{-6}	243.01	5.49	0.9910
	338	5.98	4.21×10^{-6}	237.39	5.46	0.9890

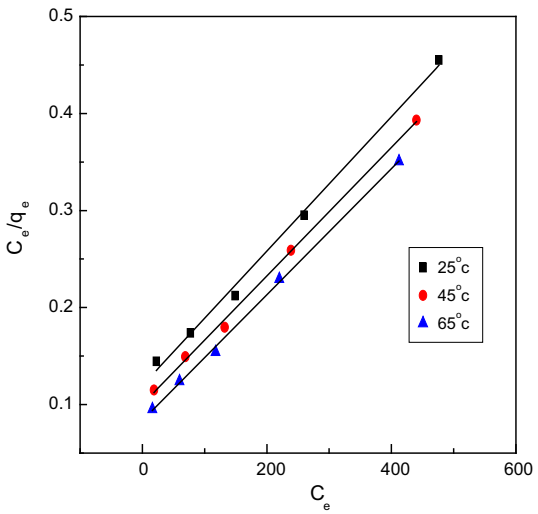

Fig. 6 Langmuir isotherm plot for the adsorption of La^{3+} onto {PASnMoP}

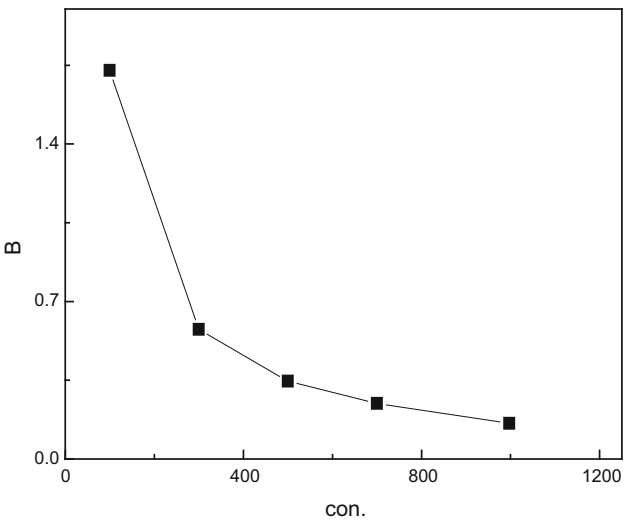

Fig. 8 Variation of adsorption intensity (R_L) with initial La^{3+} ion concentration (C_o ppm)

and, therefore, ion exchange of both La^{3+} and Sm^{3+} is favorable. From Fig. 8, we can also see that the R_L values decreased with the increasing initial concentration. This indicates that ion exchange is more favorable for the higher initial La^{3+} and Sm^{3+} concentration than for the lower one.

Freundlich isotherm is an empirical equation that encompasses the heterogeneity of sites and the exponential distribution of sites and their energies. The sorption data have been analyzed using the logarithmic form of the Freundlich isotherm as shown below:

$$\text{Log } q_e = \log K_f + \frac{1}{n} \log C_e \quad (16)$$

where K_f (mg/g) and n are Feundlich constants incorporating all factors affecting the adsorption process such as adsorption capacity and intensity of adsorption. These constants are determined from the slope and intercept of linear plot of log q_e versus log C_e, respectively.

The constants K_f and n of the Freundlich model are, respectively, obtained from the intercept and the slope of the linear plot of log q_e versus log C_e according to Figs. 9 and 10. The constants K_f can be defined as an adsorption coefficient which represented the quantity of adsorbed metal ion for a unit equilibrium concentration (i.e., $C_e = 1$). Higher values of K_f indicate higher affinity for La^{3+} and Sm^{3+}. The slope $1/n$ is a measure of the adsorption intensity or surface heterogeneity [28, 29].

The Freundlich adsorption constants evaluated from isotherms and their correlation coefficient are presented in Table 5. For $1/n = 1$, the partition between the two phases is independent of the concentration; the situation $1/n < 1$ is the most common and corresponds to a normal L-type

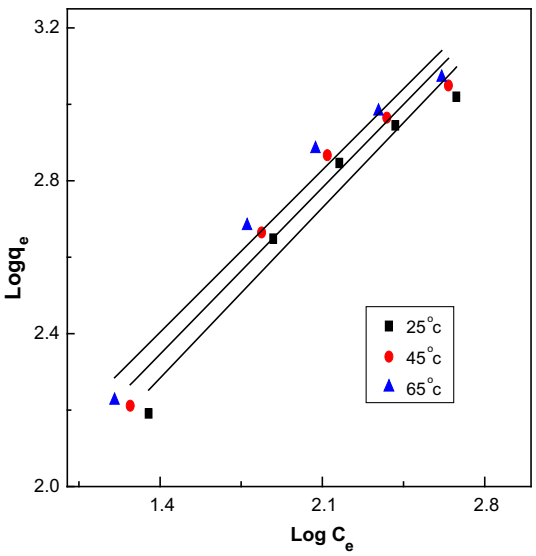

Fig. 9 Freundlich isotherm plot for the adsorption of La^{3+} onto PASnMoP

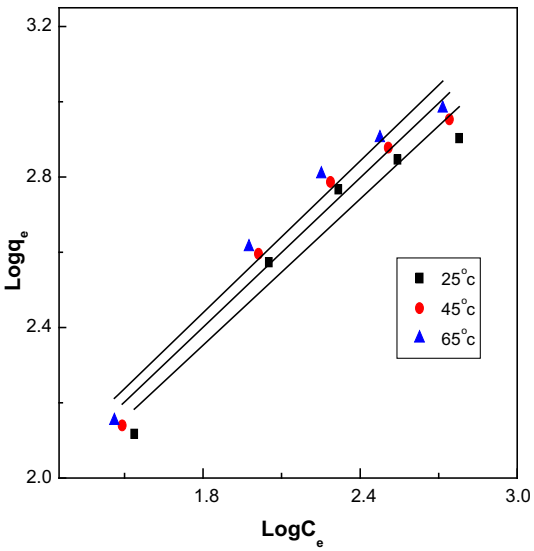

Fig. 10 Freundlich isotherm plot for the adsorption of Sm^{3+} onto PASnMoP

Table 5 Parameters of Freundlich isotherm for ion exchange of La^{3+} and Sm^{3+} on {PASnMoP}

Metal	Temp.	$1/n$	K_f	R^2
La^{3+}	298	0.636	24.66	0.946
	318	0.622	29.85	0.954
	338	0.606	35.80	0.951
Sm^{3+}	298	0.647	15.38	0.931
	318	0.662	15.84	0.951
	338	0.672	16.97	0.950

Langmuir isotherm, while $1/n > 1$ is indicative of a cooperative adsorption which involves strong interaction between the molecules of adsorbate. Values of $1/n < 1$ show favorable ion exchange of metals on ion-exchange resin, as shown in Table 5.

Kinetic investigation

The two important physicochemical factors for parameter evaluation of the adsorption process as a unit operation are the kinetics and the equilibrium. Kinetics of adsorption describing the solute uptake rate, which in turn governs the residence time of adsorption reaction, is one of the important characteristics defining the efficiency of adsorption. Hence, in the present study, the kinetics of metal removal has been carried out at 298–338°K to understand the behavior of this exchanger.

In the study, Lagergren-first-order equation and Pseudo-second-order equation were used to test the experimental data. The lagergren-first-order equation is expressed as [30, 31]:

Table 6 Comparison between adsorption rate constants, estimated q_e and coefficients of correlation associated with the Lagergren-first-order and the Pseudo-second-order kinetic models

Metal	T °K	First-order kinetic model			Second-order kinetic model				
		q_e (mg g^{-1})	$k_1 \times 10^{-2}$ (min^{-1})	R^2	h (mg g^{-1} min^{-1})	$k_2 \times 10^{-3}$ (mg g^{-1} min^{-1})	q_e (mg g^{-1})	$T_{1/2}$ (min.)	R^2
La^{3+}	298	35.54	−9.1	0.8698	5.11	7.69	81.56	15.93	0.999
	318	31.05	−13.9	0.9846	9.31	13.34	83.54	8.96	0.999
	338	22.19	−13.4	0.9959	13.77	18.95	85.25	6.18	0.999
Sm^{3+}	298	20.41	−3.1	0.9574	4.22	7.8	73.36	17.38	0.999
	318	19.27	−2.7	0.9460	4.94	8.58	75.93	15.35	0.999
	338	15.19	−1.8	0.8236	5.83	6.9	77.55	13.36	0.999

$$\ln(q_e - q_t) = \ln q_e - k_1 t \quad (17)$$

where k_1 (min^{-1}) is the rate constant of first-order adsorption, q_e is the amount of metal adsorbed at equilibrium and q_t is the amount adsorbed at time "t". Plotting $\ln(q_e - q_t)$ against "t" at (298–338) °K provided first-order adsorption rate constant (k_1) and q_e values from the slope and intercept (Table 6).

The Pseudo-second-order equation [32, 33].

$$\frac{t}{q_e} = \frac{1}{k_2 q_e^2} + \frac{1}{q_e} \quad (18)$$

The product $k_2 q_e^2$ is the initial adsorption rate "h" (mg g^{-1} min^{-1}):

$$h = k_2 q_e^2 \quad (19)$$

The half adsorption time is the time required to uptake half of the maximal amount of adsorbate at equilibrium. It characterizes the adsorption rate as well. In case of Pseudo-second-order process, its value is given by the following relationship:

$$t_{1/2} = \frac{1}{k_2 q_e} \quad (20)$$

where k_2 (mg g^{-1} min^{-1}) is the Pseudo-second-order rate constant, q_e is the amount adsorbed at equilibrium, $t_{1/2}$ is the half adsorption time and q_t is the amount of metal adsorbed at time "t". Plotting t/q_t against "t" at (298–338 °K) (Figs. 11, 12) provided second-order adsorption rate constant (k_2) and q_e values from the slope and intercept (Table 6). The values of correlation coefficient indicate a better fit of Pseudo-second-order model with the experimental data compared to the Lagergren-first-order model at all studied temperatures. The same type results were also given in same works.

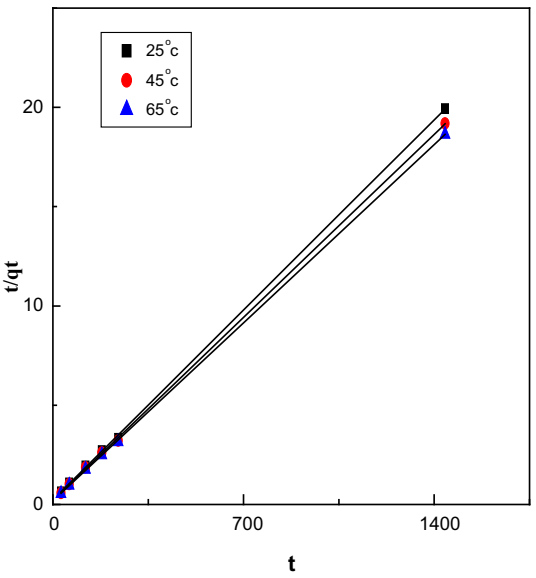

Fig. 12 Test of Pseudo-second-order equation for adsorption of Sm^{3+} from {PASnMoP} at different reaction temperatures

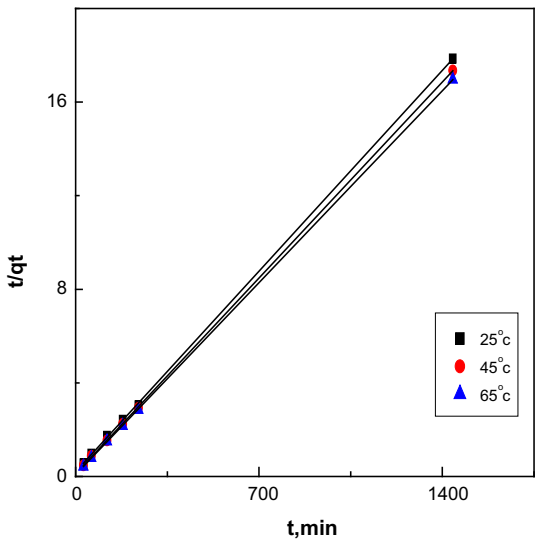

Fig. 11 Test of Pseudo-second-order equation for adsorption of La^{3+} from {PASnMoP} at different reaction temperatures

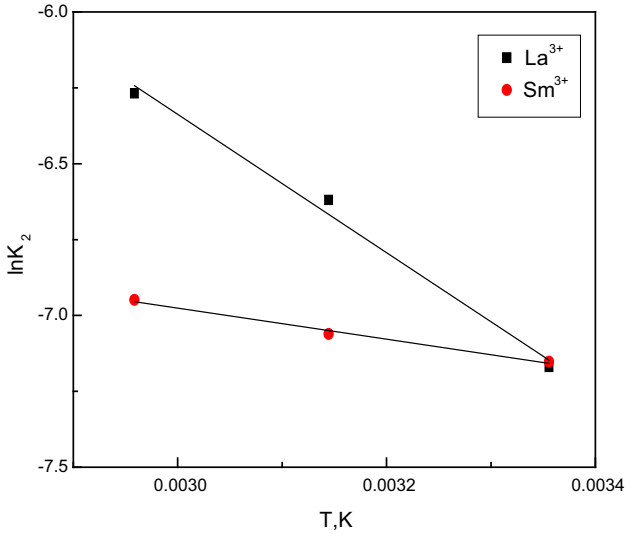

Fig. 13 Plots of Ln K vs. 1/T for adsorption of La^{3+} and Sm^{3+} ions onto PASnMoP

Table 7 Thermodynamic parameters of La^{3+} and Sm^{3+} adsorption onto {PASnMoP}

Metal	ΔH^o kJ mol^{-1} K^{-1}	ΔS^o kJ mol^{-1} K^{-1}	ΔG^o kJ mol^{-1}		
			298 °K	318 °K	338 °K
La^{3+}	18.94	4.13	17764.19	17475.8	17591.42
Sm^{3+}	4.51	45.14	17714.63	18665.5	19502.31

Thermodynamic parameters evaluation

Temperature dependence of the adsorption process is associated with several thermodynamic parameters. Thermodynamic considerations of an ion-exchange process are necessary to conclude whether the process is spontaneous or not. Thermodynamic parameters such as Gibbs free energy ($\Delta G°$), enthalpy change ($\Delta H°$) and entropy change ($\Delta S°$) can be estimated using equilibrium constants changing with temperature. The Gibbs free energy change of the adsorption reaction is given by the following Eq. (23):

$$\overline{\Delta G°} = -\mathrm{RT}\ \ln K \tag{21}$$

where R is universal gas constant (8.314 mol^{-1} k^{-1}), T is the absolute temperature (K) and $K(q_e/C_e)$ is the distribution coefficient [15, 34].

Relation between $\Delta G°$, $\Delta H°$ (enthalpy change) and $\Delta S°$ (entropy change) can be expressed by the following equation [35, 36]:

$$\Delta G^o = \Delta H^o - T\Delta S^o \tag{22}$$

Equation (22) can be written as:

$$\ln K = \frac{\Delta S^o}{R} - \frac{\Delta H^o}{RT} \tag{23}$$

where values of ΔH^o and ΔS^o can be determined from the slope and the intercept of the plot between ln K versus 1/T (Fig. 13).

The values ΔG^o, ΔH^o and ΔS^o along with relation coefficient are given in Table 7. The magnitude of ΔG^o decreased with rising the temperature; from Table 7, the values of ΔH^o were positive, indicating that the ion-exchange reaction is endothermic. This is also supported by the increase in value of uptake capacity of the adsorbent with rising the temperature.

The positive values of ΔS show the increasing randomness at the solid/liquid interface during the adsorption of La^{3+} and Sm^{3+} on PASnMoP. Obviously, it is shown from the results reported in Table 7 that the temperature affects the adsorption process of metal ion adsorption onto the resin in which the higher temperature provided more energy to enhance the adsorption rate.

Conclusion

The distribution coefficients of the prepared polyacrylamide Sn(IV) molybdophosphate (PASnMoP) have been investigated for La^{3+} and Sm^{3+} ions and the values of thermodynamic parameters were determined and the overall adsorption processes were found to be spontaneous and endothermic. The linear Langmuir and Freundlich isotherm models were used to represent the experimental data, and the experimental data could be relatively well intercept by the Langmuir isotherm. R_L values between 0 and 1.0 further indicate a favorable adsorption of La^{3+} and Sm^{3+}. By applying the kinetic models to the experimental data, it was found that the adsorption of La^{3+} and Sm^{3+} onto PASnMoP followed the Pseudo-second-order rate kinetics. The negative ΔG^o values showed that the ion exchange of La^{3+} and Sm^{3+} was spontaneous. The positive values of ΔS^o revealed the increased randomness at the solid solution interface.

References

1. Nabi SA, Naushad MU (2007) Studies of cation exchange thermodynamics for alkaline earths and transition metal ions on a new crystalline cation exchanger: aluminium tungstate and

distribution coefficient values of metal ions in surfactant media. Coll Surf A Phys Eng Asp 293:175–184
2. Nabi SA, Naushad MU, Khan AM (2006) Sorption studies of metal ions on napthol blue-black modified Amberlite IR-400 anion exchange resin. Separation and determination of metal ion contents of pharmaceutical preparation. Coll Surf A Phys Eng Asp 280:66–70
3. Nabi SA, Naushad MU, Ganai SA (2010) Preparation and characterization of a new inorganic cation-exchanger: zirconium (IV) iodosilicate: Analytical applications for metal content determination in pharmaceutical sample and synthetic mixture. Desalination Water Technol 16:29–38
4. Al-Othman ZA, Inamuddin Mu (2011) Naushad, Forward (M^{2+}–H^{+}) and reverse (H^{+}–M^{2+}) ion exchange kinetics of the heavy metals on polyaniline Ce(IV) molybdate: a simple practical approach for the determination of regeneration and separation capability of ion exchanger. Chem Eng J 171:456–463
5. Al-Othman ZA, Naushad MU, Inamuddin (2011) Organic–inorganic type composite cation exchanger poly-o-toluidine Zr(IV)-tungstate: Preparation, physicochemical characterization and its analytical application in separation of heavy metals. Chem Eng J 172:369–375
6. Al-Othman ZA, Naushad M, Ali R (2013) Kinetic, equilibrium isotherm and thermodynamic studies of Cr(VI) adsorption onto low-cost adsorbent developed from peanut shell activated with phosphoric acid. Environ Sci Poll Res 20(5):3351–3365
7. Zhou J, Duan W, Zhou X, Zhang C (2007) Application of annular centrifugal contractors in the extraction flow sheet for producing high purity yttrium. Hydrometallurgy 85:154–162
8. Qureshi M, Varshney KG (1991) Inorganic ion exchangers. In: Chemical analysis, CRC Press. Boca Ralon
9. Clearfield A (2000) Solvent extraction and ion exchanger. 18:655–678
10. Khan AA, Inamuddin, Alam MM (2005) Preparation, characterization and analytical applications of a new and novel electrically conducting fibrous type polymeric–inorganic composite material: polypyrrole Th(IV) phosphate used as a cation-exchanger and Pb(II) ion-selective membrane electrode. J Mater Res Bull 40:289–305
11. Khan AA, Alam MM (2003) Synthesis, characterization and analytical applications of a new and novel 'organic inorganic' composite material as a cation exchanger and Cd(II) ion-selective membrane electrode: polyaniline Sn(IV) tungstoarsenate. J React Funct Polym 55:277–290
12. Khan AA, Khan A, Inamuddin (2007) Preparation and characterization of a new organic–inorganic nano-composite poly-o toluidine Th(IV) phosphate: its analytical applications as cation-exchanger and in making ion-selective electrode. J Talanta 72:699–710
13. Khan AA, Paquiza L (2011) Characterization and ion-exchange behavior of thermally stable nano-composite polyaniline zirconium titanium phosphate: its analytical application in separation of toxic metals. J Desalination 265:242–254
14. El-Naggar IM, Mowafy EA, Abdel-Galil EA, El-Shahat MF (2010) Synthesis, characterization and ion-exchange properties of a novel 'organic–inorganic' hybrid cation-exchanger: polyacrylamide Sn(IV) molybdophosphate. Global J Phys Chem 1:91–106
15. Sari A, Tuzen M, Cıtak D, Soylak M (2007) Adsorption characteristics of Cu (II) and Pb(II) onto expanded perlite fromaqueous solution. J Hazard Mater 148:387–394
16. Abdel-Galil EA (2006) Chemical studies for sorption of some radionuclides on Silico(IV) titanate as cation exchanger" M.Sc. Thesis, Chemistry Dept., Fac. of Sci., Zagazig Univ
17. Abou-Mesalam MM, Shady SA (2004) Chemical in situ precipitation and immobilization technologies of radioactive liquid waste using titanium(iv) antimonate ion exchanger. Arab J Nucl Sci Appl 37:101–111
18. Clark A (1970) Theory of adsorption and catalysis. Academic Press, New York, p 54
19. Abou-Mesalam MM (2012) Evaluation of Crystalline size and Lattice Strain in Nano Particles of Transition Metals Hexacyano Ferrate. International Journal of advanced Chemical Technology 2(1)
20. Abou-Mesalam MM (2011) Hydrothermal synthesis and characterization of a novel zirconium oxide and its application as an ion exchanger. Adv Chem Eng Sci 1:20–25
21. Mishra SP, Singh UK, Tiwari D (1996) Inorganic particles in removal of toxic metal ions, IV. Efficient removal of zinc ions from aqueous solution by hydrous zirconium oxide. J Radiat Chem 210:207–211
22. Helfferich F (1962) Ion exchange. McGraw Hill, New York
23. Abou-Mesalam MM (2003) Sorption kinetics of copper, zinc, cadmium and nickel ions on synthetized silico-antimonate ion exchanger. J Coll Surf 215:205–211
24. Nabi SA, Usmani S, Rahman N (1996) Synthesis, characterization and analytical Applications Of an ion exchange material: zirconium (IV) iodophosphate. Ann Chim Fr 21:521–530
25. Shady SA (2009) Selctivity of cesium from fission radionuclides using resorcinol—formaldehyde and zirconyl—mplybdopyrophosphate as ion exchangers. J Hazard Mater 167:947–952
26. Paric J, Trago M, Medvidovic NV (2004) Removal of zinc, copper and lead by natural zeolite—a comparison of adsorption isotherms. Water Res 38:1839–1899
27. Langmuir I (1916) The constitution and fundamental properties of solids and liquids. Part I. solids. J Am Chem Soc 38:2221–2295
28. Gopal V, Elango KP (2007) Equilibrium, kinetic and hermodynamic studies of adsorption of fluoride onto plaster of paris. J Hazard Mater 141:98–105
29. Chabani M, Amrane A, Bensmaili A (2006) Kinetic modeling of the adsorption of nitrates by ion exchange resin. J Chem Eng 125:111–117
30. Agrawal A, Sahu KK (2006) Kinetic and isotherm studies of Cadmium adsorption on manganes nodule residue. J Hazard Mater 137:915–924
31. Uysal M, Ar I (2007) Removal of Cr4+ from industrial wastewaters by adsorption. Part1. Determination of optimum conditions. J Hazard Mater 149:282–291
32. Prasanna Kuma Y, King P, Prasad VSRK (2006) Equilibrium and Kinetic studies for the biosorption system of $Copper^{2+}$ ion from aqueous solution using Tectona grandis LF. leaves powder. J Hazard Mater 137:1211–1217
33. Chen CL, Li XL, Zhao DL, Tan XL, Wang XK (2007) Adsorption Kinetic, thermodynamics and adsorption studies of Th^{4+} on oxidized multi –wall Carbon nanotubes. Coll Surf A 302:449–954
34. Sari A, Mendil D, Tuzen M, Soylak M (2008) Biosorption of Cd (II) and Cr(III) from aqueous solution by moss (Hylocomium-splendens) biomass: equilibrium, kinetic and thermodynamic studies. J Chem Eng 144:1–9
35. Donat R, Akdogan A, Erdem E, Cetisli H (2005) Themodynamics of Pb^{2+} and Ni^{2+} adsorption onto natural bentonite from aqueous solutions. J Coll Interface Sci 286:43–52
36. Khani MH, Keshtkar AR, Ghannadi M, Pahlavanzadeh H (2008) Equilibrium, kinetic and thermodynamic study of the biosorption of uranium onto Cystoseriaindica algae. J Hazard Mater 150:612–618